

LA-4905-MS

UNCLASSIFIED

Copy No. **03** A



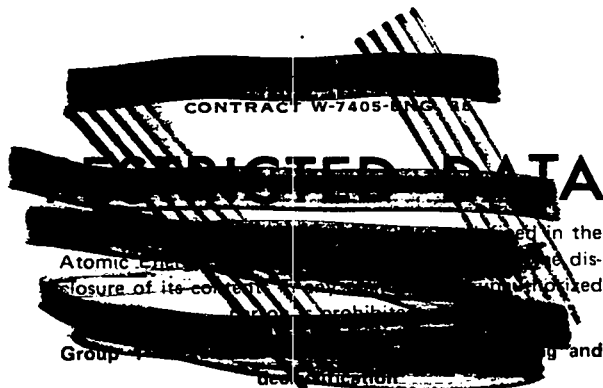
CIC-14 REPORT COLLECTION  
**REPRODUCTION  
COPY**

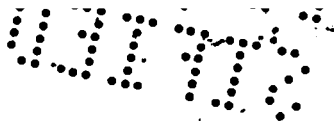
# Spheroidization and Coating of Lithium Deuteride (U)



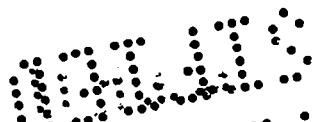
**Los Alamos**  
**scientific laboratory**  
of the University of California  
LOS ALAMOS, NEW MEXICO 87544

UNCLASSIFIED





This report was prepared as an account of work sponsored by the United States Government. Neither the United States nor the United States Atomic Energy Commission, nor any of their employees, nor any of their contractors, subcontractors, or their employees, makes any warranty, express or implied, or assumes any legal liability or responsibility for the accuracy, completeness or usefulness of any information, apparatus, product or process disclosed, or represents that its use would not infringe privately owned rights.



This document consists of 18 pages

LA-4905-MS

ATOMIC WEAPON DATA

ISSUED: April 1972

**Los Alamos**  
**scientific laboratory**  
of the University of California  
LOS ALAMOS, NEW MEXICO 87544

VERIFIED UNCLASSIFIED

Per JSW 6-18-79  
By Kolar 10-5-95

PUBLICLY RELEASABLE

Per Sandoval FSS-16 Date: 8-28-95  
By Kolar CIC-14 Date: 10-5-95

# Spheroidization and Coating of Lithium Deuteride (U)

by

H. Sheinberg  
R. E. Riley  
J. M. Taub

LOS ALAMOS NATL LAB. LIBS.  
3 9338 00407 0032

Classification changed to UNCLASSIFIED  
by authority of the U. S. Atomic Energy Commission,

Per Wilbur A. Strasser, Chief, DOC, 1/31/75  
By REPORT LIBRARY Pete Martinez, 4/11/75

UNITED STATES  
ATOMIC ENERGY COMMISSION  
CONTRACT W-7405-ENG-36

~~RESTRICTED DATA~~  
~~Atomic Energy Commission~~  
~~Office of Research and Development~~  
~~Los Alamos Scientific Laboratory~~  
~~Los Alamos, New Mexico~~

UNCLASSIFIED

**UNCLASSIFIED**

LA-4905-MS

USAF/C, Headquarters Library, Reports Section, Washington, D. C.	1-3
Manager, ALO, Albuquerque, New Mexico	4
Lawrence Livermore Laboratory, Livermore, California	5-6
Sandia Corporation, Albuquerque, New Mexico	7
Military Liaison Committee, Washington, D. C.	8
Director, Defense Research and Engineering, Washington, D. C.	9
Headquarters, Defense Nuclear Agency, Washington, D. C.	10-11
Defense Nuclear Agency Field Command, Kirtland AFB, New Mexico	12-14
Commanding General, Army Combat Developments Command, Fort Belvoir, Virginia	15-16
Commanding General, Army Materiel Command, Washington, D. C.	17
DCS/Operations, Army, Washington, D. C.	18
Chief, R&D, Army, Washington, D. C.	19
Naval Ordnance Systems Command, Washington, D. C.	20
Chief of Naval Operations (OP-75), Washington, D. C.	21
DCS/Research and Development, Headquarters, USAF, Washington, D. C.	22
Director, Air Force Weapons Laboratory, Kirtland Air Force Base, New Mexico	23-25
Los Alamos Report Library	26-40

**UNCLASSIFIED**

UNCLASSIFIED

## SPHEROIDIZATION AND COATING OF LITHIUM DEUTERIDE

by

H. Sheinberg, R. E. Riley, and J. M. Taub

## ABSTRACT

The feasibility of several processes for producing 90- to 110- $\mu$ -diam spherical lithium deuteride particles was investigated. The process adopted was gravity flow of angular particles through a 3-1/2-in.-long tube resistance heated to  $\sim 1150^{\circ}\text{C}$ . Spherical particles thus produced had a composition of  $\sim \text{LiD}_{0.79}$ , but composition was restored to  $\sim \text{LiD}_{0.94}$  by cycling the particles between 350 and  $500^{\circ}\text{C}$  in purified  $\text{D}_2$ . Particles were coated with  $\sim 5 \mu$  of aluminum by vaporizing aluminum from a heated tungsten filament onto particles contained in a vibrating pan beneath it.

## I. Introduction

The Los Alamos Scientific Laboratory (LASL) and other laboratories are engaged in experimental and theoretical efforts based on the concept of initiating thermonuclear fusion reactions by concentrating pulsed laser energy on a small pellet of deuterium-tritium (D + T) fuel. Focusing short-pulse laser energy on a small amount of material can produce energy concentrations far exceeding those attainable by nonnuclear means. If large enough pulsed lasers can be developed, it will be possible to initiate large thermonuclear energy releases. The particular significance of such a development for space propulsion lies in the potentially very small mass of the energy source. It has been demonstrated that the performance of a pulsed propulsion system is a strong inverse function of the mass of the individual unit in which the energy is produced.<sup>1</sup>

An objective of the thermonuclear burn phase of the Laser Program is the study of energy interaction of a laser beam with lithium deuteride (LiD) or lithium deuteride-tritide (LiDT). Calculations indicate that maximum deuterium-tritium burn efficiency is achieved using a spherical  $\sim 100\text{-}\mu$ -diam LiDT particle, and that energy coupling with such a particle is increased if it is coated with a thin layer of a higher electron density element such

as aluminum which acts as a pusher. An impervious aluminum coating on the LiDT particle may also function as a pressure vessel to retain decay products from the tritium.

The Powder Metallurgy Section of the LASL Materials Technology Group, CMB-6, was requested to produce small amounts of 90- to 110- $\mu$ -diam spherical particles of LiD coated with  $\sim 5 \mu$  of aluminum using a process compatible with translation of LiDT or LiT. During investigation of processes for production of this material, work at Mound Laboratory indicated that an isotopic exchange of LiD with  $\text{T}_2$  to yield LiDT in relatively short times was practical. Our investigations were altered to accommodate this information.

The low density of LiD (and/or LiDT), combined with its high deuterium or deuterium-tritium atomic concentration per cubic centimeter and its high thermal and radiation stability, makes it very interesting as a thermonuclear fuel material. Because of its similarity with LiD, lithium hydride (LiH) could be used as a stand-in material for process development. There are differences in such physical properties as density and lattice parameters of these face-centered compounds. The heats of formation of LiD and LiT are more negative than that of LiH, and the dissociation pressures are greater than that of the corresponding hydride because of an absolute entropy of

UNCLASSIFIED

UNCLASSIFIED

the deuterium gas which leads to a higher entropy of formation.

Both lithium hydride and lithium deuteride are very reactive materials, and this reactivity creates considerable difficulty in the processing and evaluation of fine particulates. When heated, LiH decomposes into Li + H<sub>2</sub>, both of which are strong reducers. Lithium hydride partially dissociates at its melting point with a dissociation pressure of 27 Torr;<sup>2</sup> continuous removal of hydrogen effects complete dissociation.

Large lumps of lithium hydride can be briefly handled in low-humidity air because a thin layer of hydroxide forms rapidly and drastically reduces the rate of reaction. Finely divided powder with its high specific area and low thermal conductivity is, of course, more susceptible to pyrophoric behavior than is massive material. The fine powders (< 100 mesh) react instantly with small amounts of water or water vapor, sometimes with explosive violence, and the liberated H<sub>2</sub> ignites spontaneously.

Lithium hydride is produced by passing hydrogen into molten lithium; solidification of the hydride (accompanied by ~18% shrinkage) produces a nearly stoichiometric massive form containing a small amount of free lithium metal.

It has been reported that the hydride may be dispersed in ethers, unreactive alkyl halides, esters without a hydrogen, and tertiary amides; and that LiH is compatible with many plastic monomers and polymers. However, bubble formation is caused when only traces of moisture, peroxides, or acidic materials are present.<sup>3</sup> This bubble formation has prevented development of a technique for metallographic examination of uncoated LiH powder.

The program at CMB-6 was broken down into several concurrently active phases. Phase I consisted of experiments on spheroidization of LiH and LiD in the desired particle-size range. Phase II involved experiments on rehydriding and redeuteriding the spheroidized powders to restore the hydride or deuteride lost during spheroidization. Phase III efforts have been devoted to perhaps the most difficult task, laying down a uniform coating of aluminum metal on the spheroidized and redeuterided particles. Phase IV is an evaluation of the progress to date to dictate future efforts which are also described here.

## II. Particle Spheroidization

Five processes for preparation of the required spherical powders were briefly investigated; normal LiH was used as a stand-in for LiD.

A. Spheroidization and Hydriding of Metallic Lithium in Oil. The equipment for this process consisted of a

Brookfield counter-rotating high-shear, high-cutting-action stirrer with speeds variable from 100 to 20,000 RPM; a hot plate; a 500-cm<sup>3</sup> Pyrex beaker containing Primol 355 (a clear hydrocarbon oil); and a submerged perforated copper tube in the bottom of the beaker. The oil was heated to ~200°C and stirred; hydrogen was admitted through the submerged tube. Large lumps of lithium metal were dropped into the oil, the mixture was stirred, and argon was admitted through a perforated tube at the top of the beaker to provide an inert-atmosphere blanket.

We prepared four batches of ~20-cm<sup>3</sup> spherical lithium (or LiH) in this manner. One batch was heated and stirred for 30 min. X-ray diffraction showed two phases, LiH, and, predominantly, lithium. It did appear, however, that the stirrer speed could be adjusted to yield a product with most of its particles in the required size range.

This method has several advantages: (1) it requires no material preparation, (2) it is a low-temperature process, (3) it is easy to scale up, (4) there are minimal compatibility problems, and (5) the principal variables are rate of stirring and hydriding time, both of which are controllable. Disadvantages include (1) the required removal of oil from the finished product, (2) the separation of the required size fraction from the spheroidized product, (3) the probable long-term processing for nearly stoichiometric LiD, and (4) the impracticality if direct translation to LiT or LiDT is required.

B. High-Pressure Atomization of Molten Lithium Hydride. The high-pressure atomization process involved use of inert-gas pressure in a steel container heated to ~800°C to force the molten LiH in the container through an orifice and an atomizer plate into an attached 12-in.-long steel settling chamber, using countercurrent flow of argon, as shown in Fig. 1. Interchangeable atomizer plates consisted of a conical cavity having an ~1/4-in. major-diameter inlet, with four 0.06-in.-wide, 0.06-in.-deep tangential slots at the inlet diameter and outlet holes varying from 0.040 to 0.090 in. in diameter. Both sodium chloride and sodium potassium-carbonate eutectic salts were used as a stand-in for LiH to minimize compatibility problems and hazards in case the pressurized vessel ruptured. Temperature, pressure, and orifice size were varied, but only a few cubic centimeters of spherical particles were produced.

An advantage of this process is that the feed material need not be preconditioned, but disadvantages are that (1) a relatively high pressure system is required, (2) atomizer temperature and material flow must be very accurately controlled, (3) considerable experimentation is required to correlate atomizer design with product

UNCLASSIFIED

UNCLASSIFIED

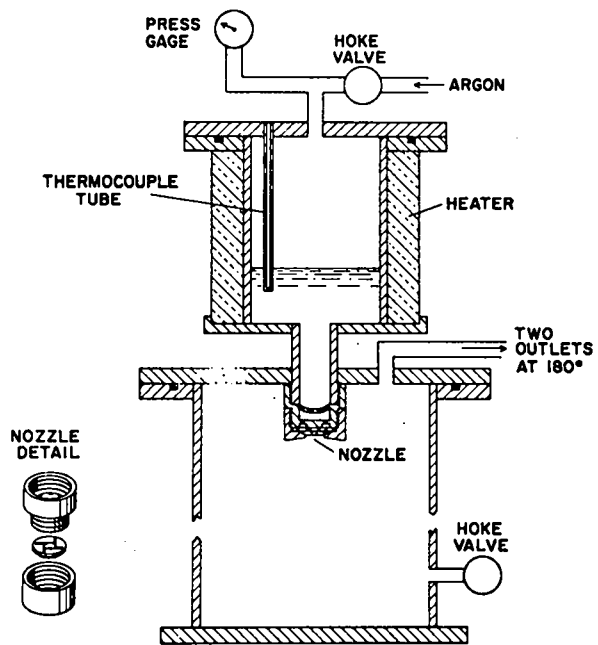


Fig. 1.

High-pressure atomization chamber and nozzle detail.

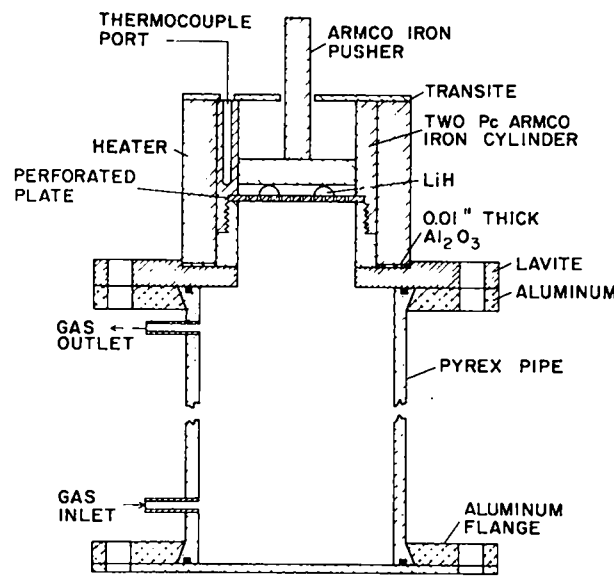


Fig. 2.

Apparatus for discharge of LiD through perforated plate.

characteristics, (4) the final product will probably have a wide size distribution, and (5) the method does not seem practical if direct translation to LiT or LiDT is required.

**C. Discharge of Molten Lithium Hydride Through a Perforated Plate.** This process involved heating LiH to slightly above its melting point in a 1.75-in.-diam ARMCO iron cylinder and forcing the molten material through a perforated plate using a loose-fitting ARMCO iron piston on top of the LiH. The equipment, shown schematically in Fig. 2, was installed in an argon-atmosphere glovebox.

The LiH, when molten, was forced through 64 0.008-in.-diam holes in a plate on which it rested into a 10-in.-long glass settling pipe. We found that close control of plate and LiH temperature is required, and that the temperature should barely exceed the melting point of the material to prevent formation of stringers or agglomeration of the spherical droplets. We obtained ~ 8 cm<sup>3</sup> of product using this setup. A new perforated plate with 121 0.005-in.-diam holes increased the capacity and provided a product with ~ 30% of the particles in the desired size range. Figure 3 shows the particles produced by this process.

Advantages of this process are that (1) feed material need not be preconditioned, (2) operating temperature is only slightly above the melting point so that hydrogen or deuterium loss is minimized, and (3) simplicity of equipment permits scale-up by multiplicity of units.

Disadvantages are that (1) the equipment is incompatible with molten LiD, (2) output per unit is low, (3) accurate and uniform perforated plate and lithium temperature is required, and (4) preliminary experiments yielded a wider than expected particle-size distribution.

**D. High-Pressure Extrusion with Subsequent Spheroidization.** This process involves low-temperature extrusion of 0.005-in.-diam LiD wire, cutting the wire into ~ 0.005-in. lengths, and individually melting these rods. Possibly a die and cutter assembly could be designed so



Fig. 3.

Particles produced using the perforated-plate technique. 50X.

UNCLASSIFIED

that a synchronized blade would cut the extruded material to correct length as it emerged from the extrusion nozzle. The principal advantage of this process is that it should produce, on spheroidization, particles of the same size.

A few ~1-1/2-in. lengths of sodium chloride, used as a stand-in for LiD, were extruded using an available 0.187-in.-i.d. hardened steel die and a 0.0075-in.-i.d. modified wire-drawing die as a nozzle at ~300°C and 50 tsi. We used commercial high-purity -50 mesh sodium chloride as feed material. Efforts to extrude -50 mesh LiH in this die at 450°C failed; the extremely high extrusion ratio and reaction of LiH with the nozzle were the probable primary causes of failure. We used 0.093-in.-i.d. hardened steel die and a nominal 0.005-in.-i.d. ZrO<sub>2</sub>-lined nozzle for additional attempts to extrude -50 mesh LiH at 50 tsi and 450 to 550°C. It appeared that using LiH extruded with low extrusion ratios as feed material for extrusion with successively smaller extrusion ratios would offer only a measure of success.

It also appeared that the principal uniform-size prespheroidized particle advantage would be outweighed by the magnitude of the following disadvantages: (1) the final feed material requires considerable preconditioning, (2) cutter speed must be very accurately synchronized with extrusion punch travel and the temperature of the cutter blade must be accurately controlled to prevent chipping, and (3) considerable experimentation with temperature and pressure will probably be required to produce the final-size, defect-free extrusion.

**E. Gravity Flow of Powder Through a Heated Drop Tower.** We have used a drop-tower technique to produce LiH and LiD spheres. Essentially, this technique consists of dropping LiH particles at a controlled rate, vertically, through a hot zone where they melt to form spheres that solidify and cool while falling free. The spheres collect in a receiver at the bottom of the drop tower in which a flow of argon provides an inert atmosphere. Both induction-heated and resistance-heated towers have been used to produce spherical LiH and LiD particles. Figure 4 is a schematic of a resistance-heated drop tower and its accompanying feed reservoir.

Use of the drop tower has been the most successful process to date. Advantages of this process are (1) simplicity of equipment, (2) capability of scale-up in either size or multiplicity, and (3) ready adaptation to continuous processing. Potential disadvantages are (1) probable loss of hydrogen or deuterium unless equipment is pressurized, (2) required preconditioning of feed material, and (3) probable need for close control of susceptor temperature and residence time in the heated zone to produce defect-free spherical particles. However, we feel that these disadvantages are surmountable and subject to control.

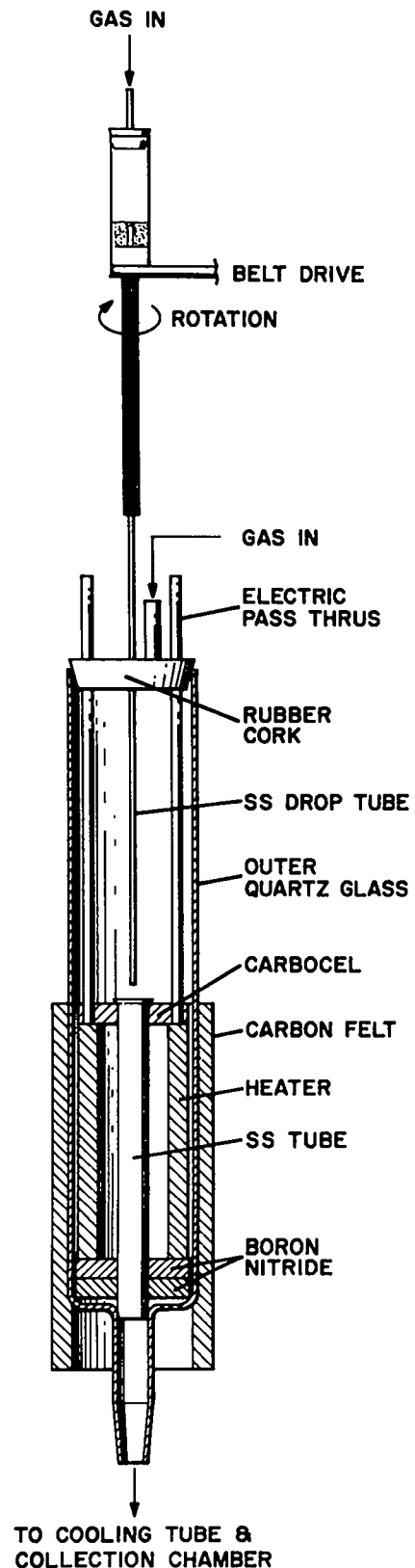


Fig. 4.

*Resistance-heated drop tower and feed reservoir.*

UNCLASSIFIED



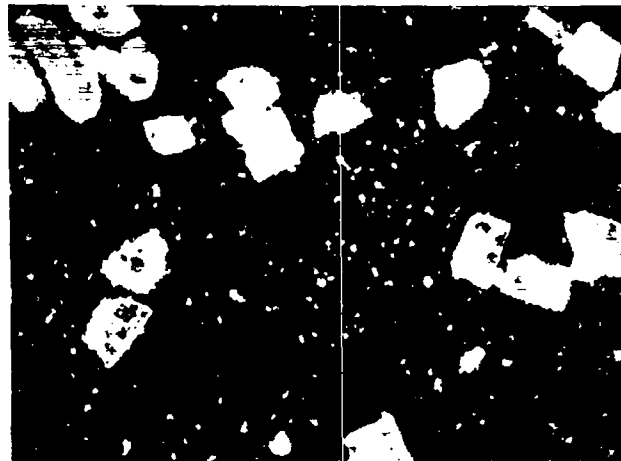
Normal LiH and LiD from Oak Ridge National Laboratory or commercial sources are usually supplied in the form of 1/8- to 1-1/2-in. irregular lumps. These lumps are hand crushed in an argon-atmosphere glovebox to maximize the yield of -100 +170 mesh United States Standard (USS) powder. The typical yield of powder in this size range is  $\sim 30\%$ . The fine powder is saved and part of it is used as a "getter" in the glovebox. The particle-size spread is subsequently reduced to 95 to 140  $\mu\text{m}$  by using specially prepared screens.

The first drop tower had an induction-heated 5/8-in.-i.d. by 3-in.-long tubular graphite susceptor as its heat source. Hand feeding LiH powder through the tower operated at 1200°C yielded  $> 90\%$  spherical particles, but 20 to 30% of them seemed to contain bubbles or cavities. Lower tube temperatures yielded much lower percentages of spherical particles, and some of these particles contained cavities. Because of the difficulty in maintaining a uniform temperature throughout its length, we abandoned the induction-heated tube in favor of a resistance-heated stainless steel tube.

We constructed and tested a resistance-heated drop tower. Tubular Kanthal-wound heating elements were used to heat a 11/16-in.-i.d. by 8-in.-long stainless steel drop tube. We made six runs on this tower to determine the optimum operating conditions. At drop-tube temperatures of 850°C and below, we collected fewer than 50% spheres, and of these up to 30% had cavities. At above 850°C 95 to 98% of the particles were spheroidized, but more than 50% of the spheres were hollow or contained easily observable cavities.

We installed new apparatus with a 3-1/2-in.-long hot zone, heated by clam-shell resistance heaters and with a  $\text{ZrO}_2$  insulator to protect the heater coils from lithium or LiD vapor. We installed a mechanically operated powder-feed system to eliminate the variations inherent in a manual system. Work with LiH indicated an optimum temperature of 1100°C that produced a yield of  $\sim 50\%$  spheres with few visible defects. This temperature proved too low for LiD, probably because of the difference in heat capacity of the two materials. Current work indicates that the temperature range for producing a high yield of spherical LiD powder with low visual defect concentration is 1125 to 1175°C. Figure 5 shows feed LiD powder and the spheroidized and classified LiD powder. Figure 6 shows scanning electron micrographs of these powders.

We have classified spheroidized LiH and LiD powders on an adjustable inclined vibratory table to separate spherical from nonspherical particles. Typically, one pass on this table removed better than 90% of the nonspherical particles, and a second pass seemed to remove  $\sim 99\%$  of them. However, this process does entrain some of the spherical powder with the nonspherical powder, and the product yield is accordingly reduced.



As-crushed and screened material -100 +140 mesh,  $\text{D}_2$  content 21.83 wt%.



As-spheroidized at 1150°C in argon atmosphere,  $\text{D}_2$  content 19.34 wt%.

Fig. 5.

LiD raw material and spheroidized LiD particles. 50X.

### III. Rehydriding and Redeuteriding of Spheres

Of major importance is the  $\text{H}_2$  and  $\text{D}_2$  content of the spherical particles. Recorded in Table I are  $\text{H}_2$  and  $\text{D}_2$  analyses for some spheroidized and classified powders. These same powders were rehydrided or redeuterided at 400°C for 50 h in purified  $\text{H}_2$  or  $\text{D}_2$ .

Group CMB-1 determined hydrogen or deuterium by burning three  $\sim 100\text{-mg}$  samples in a stream of purified oxygen and weighing the water produced. The data indicate a considerable greater  $\text{H}_2$  loss with increasing spheroidization temperature. Note that the rehydriding for 50 h at 400°C restored approximately half of the  $\text{H}_2$

UNCLASSIFIED



Crushed and screened LiD -100 +140 mesh.



Screened LiD spheroidized at 1150°C.

Fig. 6.

Crushed and screened, and spheroidized LiD particles. 100X.

lost during spheroidization, but these conditions were not optimum for restoration of the  $D_2$ . We believed that use of a higher temperature would promote  $D_2$  gain and that temperature cycling might also promote  $D_2$  gain as well as prevent sintering of the particles. We placed a 0.4-g batch of the classified spherical LiD particles containing 19.34 wt%  $D_2$  in an electrobalance chamber in static  $D_2$  atmosphere. The sample temperature was cycled between 300 and 500°C three times during a 6-h run; chemical analysis indicated a final  $D_2$  content of 20.65%. It appeared that temperature cycling and use of 500°C

TABLE I

## HYDROGEN AND DEUTERIUM ANALYSES OF RAW AND PROCESSED POWDERS

<u>Lithium Hydride</u>	<u>H<sub>2</sub> Wt%</u>
Raw material	12.62
Spheroidized at 1200°C, Ar	9.23
Spheroidized at 1200°C, Ar - 10% H <sub>2</sub>	9.91
Spheroidized at 1100°C, classified	11.41
Spheroidized at 1125°C, classified	10.89
Spheroidized at 1125°C, classified rehydrated	11.67

<u>Lithium Deuteride</u>	<u>D<sub>2</sub> Wt%</u>
Raw material	21.83
Spheroidized at 1150°C, classified	19.34
Spheroidized at 1150°C, classified, redeuterided	19.68

maximum temperature would allow reintroduction of  $D_2$  to replace most of that lost during spheroidization. We expect that isotopic exchange using  $T_2$  instead of  $D_2$  will be most favorable for production of LiDT powder at this stage, when the powder is substoichiometric. Figure 7 shows spheroidized, classified LiD after redeuteriding. Note that the particles appear much smoother after this operation. The particles were light purple-grey to dark purple and gold before redeuteriding, possibly because of the substoichiometric composition. After redeuteriding, they were almost transparent and colorless.

We made two redeuteriding runs on 10-g batches of a new lot of spheroidized, shape-classified LiD spheres.

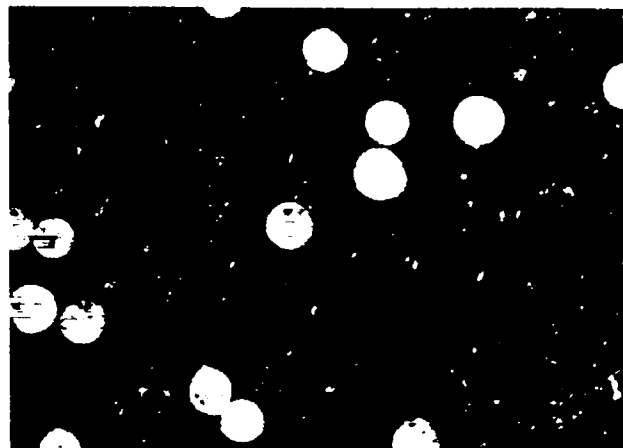


Fig. 7.

Redeuterided LiD particles. 50X.

UNCLASSIFIED

UNCLASSIFIED

We cycled one batch in 600-Torr purified  $D_2$  between 325 and 500°C for six cycles over a period of 7 h, and thermally cycled the second batch between the same temperatures for 12 cycles in 13 h. Composition of the raw material, classified spherical powder, and redeuterided material was as follows:

Raw material	$LiD_{0.98}$
Spheroidized powder	$LiD_{0.79}$
Redeuterided 6 cycles	$LiD_{0.90}$
Redeuterided 12 cycles	$LiD_{0.94}$

We have thus established that the composition of the spheroidized powder can be improved to approach that of the starting feed material.

Group CMB-1 determined both deuterium and lithium in the above samples. They performed the lithium analysis by dissolving two weighed 500-mg portions from each sample in distilled  $H_2O$ , diluting to volume, and titrating two 20-ml aliquots from each portion with 0.1N HCl to a phenolphthalein end point.

#### IV. Coating Spheroidized Particles with Aluminum

Development of a uniform  $\sim 5\text{-}\mu\text{m}$  coating of aluminum on the spheroidized and rehydrided or redeuterided particles is regarded as the most difficult phase of this program. Preliminary efforts to develop such a shell involved chemical vapor deposition (CVD) of aluminum onto the particles in a fluidized bed by thermal decomposition of tri-isobutylaluminum. After some 14 fluid-bed experiments failed to produce coherent coatings on stand-in carbon and glass spheres, we abandoned this technique in favor of the simpler physical evaporation of aluminum in a high vacuum from a resistance-heated source. The main difficulty envisioned in this technique was that of obtaining a thick, uniform coating of aluminum on all particles.

Spheres of LiH and LiD produced by the drop-tower technique were coated with aluminum by vacuum evaporation. The spheres were spread on a pan that was vibrated during the coating. The 99.9% purity aluminum was evaporated by a resistance-heated tungsten filament in  $\sim 10^{-4}$ -Torr vacuum. Evaporation of aluminum in this manner is a line-of-sight type of operation, and only a little of the total aluminum evaporated reaches the particles to be coated.

The spheres were coated with a minimum of three layers of aluminum. The coating time was dictated by the life of the tungsten filaments. We submitted samples from selected batches for metallography and weight-gain experiments in a high-humidity argon atmosphere. The humidity tests were run in a thermo gravometric-analysis

(TGA) balance setup. The TGA tests showed that the coated spheres were completely hydrolyzed in less than 48 h. In the room-temperature,  $H_2O$ -saturated, argon environment, the reaction rate for uncoated LiH spheres was 0.10 g/h/g. The rates for two batches of coated spheres were 0.084 and 0.090 g/h/g. Metallography indicated that these coatings were nonuniform and generally less than 5- $\mu\text{m}$  thick.

These preliminary vacuum-coating experiments were conducted in a commercial evaporation apparatus. Work was discontinued on this apparatus which was needed for another program.

We built an evaporation unit to accommodate resistance- or induction-heated evaporation crucibles made from 50%  $TiB_2$ -50% BN. Initially the aluminum evaporation in this study appeared promising; however, the vacuum system was unable to hold the pressure in the range required for aluminum deposition. The coatings produced were dark. We rebuilt the apparatus and adapted it to an existing high-capacity vacuum system. A 7.5-kW, 10-kHz motor generator power source was used to induction heat a  $TiB_2$ -BN crucible containing aluminum. This crucible was held inside a quartz tube mounted on a 12-in.-i.d. by 10-in.-high brass can. The LiD powder was contained in a 6-in.-diam pan within the can and under the crucible. The pan containing the LiD could be simultaneously rotated and vibrated during evaporation of the aluminum. Initial experiments in this apparatus produced a dark gray to black coating, although the pressure was less than  $10^{-4}$  Torr throughout the coating run.

We made a series of evaporation runs in this unit to establish the effect on coating thickness and structure of three parameters: distance of substrate from crucible, crucible temperature, and coating time. We substituted  $ZrO_2$  disks, 1-in. in diam by 1/8-in. thick, for the LiD powder to facilitate metallographic preparation and coating examination. Table II shows the deposition conditions and calculated coating thicknesses.

From geometric considerations, assuming a point evaporation source, the aluminum coating thickness should quadruple when the source-to-substrate distance is halved. Departure from this relationship, as noted in the Table, is due to slight pressure variations between runs, lack of a point evaporation source, and splatter of aluminum droplets at the very short source-to-substrate distance.

Metallography of the coatings showed good agreement between the calculated and measured average coating thickness, as is shown in Fig. 8. The aluminum coating seemed to have a layered, nonporous structure, and closely followed the surface contours of the porous  $ZrO_2$  substrate and appeared bonded to it. There was considerable variability in coating structures, even among deposits

TABLE II

EVAPORATION OF ALUMINUM ON ZrO<sub>2</sub> DISKS

Disk	Evaporation Temp (°C)	Source-to-Substrate Dist (in.)	Time (min)	Calculated Al thk (μm)	Color, Texture
ZrO <sub>2</sub> -1	1250	7	30	1.7	tan, smooth
2	1250	4	30	11.4	dark gray, smooth
3	1250	7	60	4.3	dark gray, smooth
4	1250	4	60	30.3	black, smooth
5	1400	4	15	46.9	dark gray, rough
6	1400	4	30	53.9	dark gray, rough
7	1400	7	15	7.6	tan, smooth
8	1250	10	60	1.4	light, tan, smooth
9	1300	6	30	7.9	dark gray, smooth
10	1200	3	60	---	light gray, splattered
11	1200	3	30	3.3	light gray, coarse
12	1200	3	60	33.7	light gray, coarse
13	1200	4	30	13.1	dark gray, smooth
14	1200	4	60	18.4	dark gray, smooth
15	1250	4	30	33.5	dark gray, smooth
16	1300	4	15	16.5	light gray, smooth
17	1300	4	30	64	medium gray
18	1300	4	60	52.5	dark gray, rough
19	1300	6	60	14.0	black, smooth
20	1400	7	30	38.6	medium gray, rough

made under the approximately same conditions. For example, three deposits made at 1300°C with a 4-in. evaporator-to-substrate distance varied in microstructure from very porous to dense, as is shown in Fig. 9. Most of the deposits were very rough and nodular, although a few were relatively smooth and even. Unfortunately, there seems to be no rigid correlation of coating conditions with these smooth, dense coatings. The dark or black surface observed previously during powder coating was also present on some disk coatings deposited at evaporation distances of < 6 in. The dark layer was apparently formed during the final stage of deposition as evidenced by its position; however, it was as much as 20 μm thick, or up to half the coating thickness.

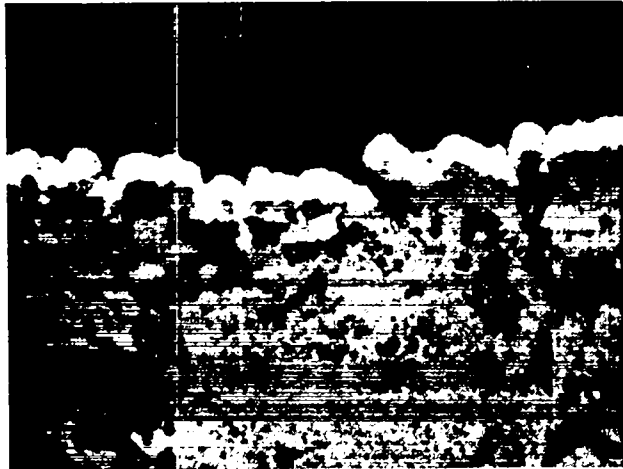
We made two aluminum evaporation runs at 1300°C, one using a tungsten crucible to contain the molten aluminum and one using a graphite crucible. Both deposits exhibited dark gray surfaces, indicating that the dark surfaces observed previously were not due to reaction of aluminum with the TiB<sub>2</sub>-BN crucible. The graphite crucible was badly attacked by molten aluminum during the run.

Development of a semicontinuous aluminum feed evaporator was conducted in another vacuum chamber.

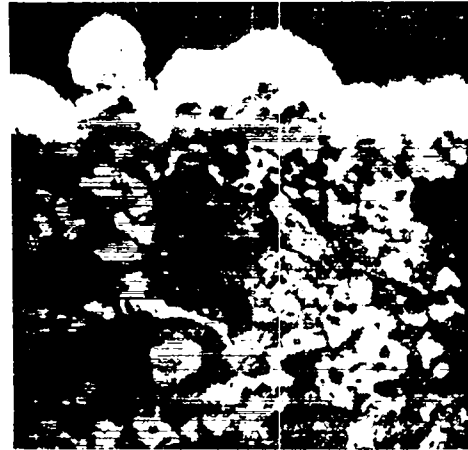
The feasibility of evaporating a 1/4-in.-diam, 7-in.-long aluminum rod from an induction-heated TiB<sub>2</sub>-BN crucible was demonstrated. This was approximately seven times the aluminum capacity of the system used for the coating experiments with the ZrO<sub>2</sub> disks.

Experimentation with diversely shaped vibrator pans (vibrated by external vibrators) containing the LiD spherical powder showed that pans with a small-radius hemispherical bottom provided excellent powder circulation. We built a container of this type with provision for water cooling for use with a semicontinuous aluminum evaporation system.

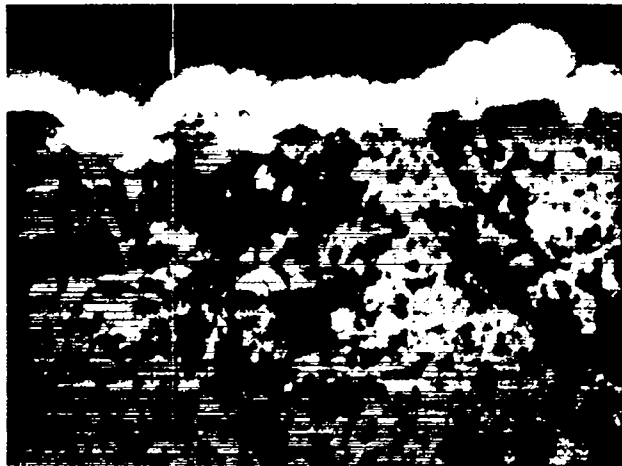
We made one run to coat redeuterated LiD spheres. We used semicontinuous aluminum feed to the evaporation crucible, and contained the LiD in a water-cooled, vibrated, hemispherical-bottomed pan. The evaporation temperature was 1250°C, and the run continued for 1-1/2 h. Part of the powder was well coated after the run, but most of it was uncoated because agglomeration of the LiD began soon after coating started. We modified the apparatus further to provide continuous powder circulation. This did minimize agglomeration during subsequent runs.



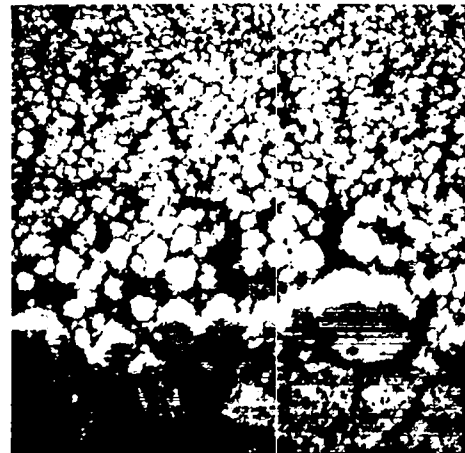
60-min coating time.  
 Calculated thickness, 14.0  $\mu$ .  
 Average observed thickness, 15  $\mu$ .



15-min coating time.



30-min coating time.  
 Calculated thickness, 7.9  $\mu$ .  
 Average observed thickness, 8  $\mu$ .



30-min coating time.



60-min coating time.

Fig. 8.

Aluminum coating on  $ZrO_2$  disks at 1300°C with 6-in. evaporator-to-substrate distance. 500X.

A second run made with a modified pan yielded a tightly agglomerated powder mass, probably because of too fast an evaporation rate. We replaced the modified water-cooled pan with an aluminum pan (attached to an internally mounted syntron vibrator) that was covered with aluminum foil so that only the center half of the pan area was exposed to the heated  $TiB_2$ -BN crucible and aluminum evaporant. A 10-min evaporating run terminated by thermocouple failure proved that use of this pan

Fig. 9.

Aluminum coating on  $ZrO_2$  disks at 1300°C with 4-in. evaporator-to-substrate distance. 500X.

without water cooling was satisfactory. Eliminating the water-cooling appendages greatly improved powder motion and vibration. However, only  $\sim 80\%$  of the  $\text{LiD}_2$  was coated, and reaction of the uncoated particles with the mounting resin prevented metallography of this material. A subsequent 1/2-h run at  $1300^\circ\text{C}$  in this partially covered pan yielded a product with  $> 95\%$  of the particles coated with aluminum; however, this material reacted with the metallographic mounting material, indicating that the coating was permeable or did not completely cover the particles. A third run in the covered aluminum pan with a reduced charge was terminated after  $\sim 10$  min at  $1300^\circ\text{C}$  when the  $\text{LiD}$  powder adhered to the bottom of the pan.

Because of the problems in getting a reproducible bright coating using the  $\text{TiB}_2$ -BN evaporator, we fabricated equipment to feed 0.080-in.-diam 99.999% pure aluminum semicontinuously onto a resistance-heated tungsten filament using the existing vibrating aluminum pan and vacuum system. This equipment is shown schematically in Fig. 10. Spherical  $\text{LiD}$  powder coated for  $\sim 65$  min in this apparatus did not react with the metallographic mounting material, indicating that it had a protective aluminum coating. When using the small heated-tungsten filaments, it was not necessary to cover part of the pan to prevent overheating.

We made three coating runs with the filament heated to  $\sim 1650^\circ\text{C}$  using coating times of 70, 75, and

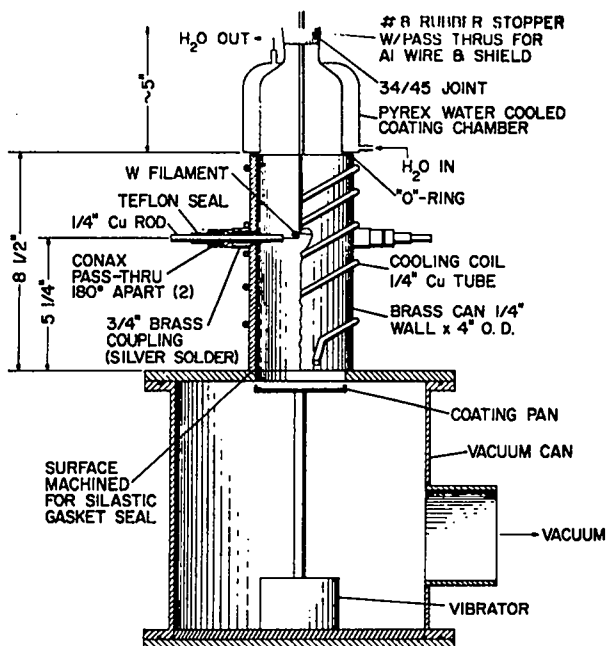


Fig. 10.  
Aluminum coating apparatus.

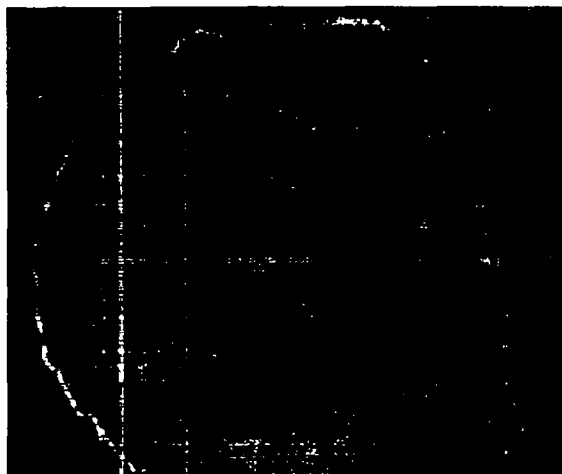
126 min. Metallography of the aluminum-coated powders indicated a solid, fairly continuous  $\sim 1$  to  $2\ \mu\text{m}$  of aluminum coating on the particles coated for 70 and 75 min, and a 3- to  $5\text{-}\mu\text{m}$ -thick coating for the 126 min coating time. A coated particle from each of these runs is shown in Fig. 11.

Radiography of the particles coated for 126 min, as shown in Fig. 12, revealed dense but irregular aluminum coatings and also revealed internal flaws and variation in structure of the  $\text{LiD}$  particles. Microscopy revealed considerable surface roughness. We therefore deemed it necessary to improve the quality and uniformity of both the surface structure and coating of the  $\text{LiD}$  particles.

Because imperfect aluminum coating on the reactive  $\text{LiD}$  causes reaction with the metallographic mounting materials, experiments to optimize vaporization coating conditions used shape-classified glass beads approximating the desired size of  $\text{LiD}$ . We made a series of coating runs with varied filament temperature, coating time, and aluminum feed-wire diameter. Filament temperature was kept at  $1650$  or  $1725^\circ\text{C}$ , and no significant effect of this variable was observed. Substituting 0.020-in.-diam wire for the 0.080-in.-diam wire used in previous experiments resulted in considerably smoother and more uniform coatings. Figures 13 and 14 are scanning electron micrographs of beads coated using the 0.080- and 0.020-in.-diam aluminum wires, respectively. Sixty-minute runs with the larger diameter wire yielded average coating thicknesses in approximately the desired range, as shown in Fig. 15, but coating thickness was nonuniform. A uniform, but only  $\sim 1$ - to  $2\text{-}\mu\text{m}$ -thick coating resulted from 120-min runs with the finer wire. We believe that a mechanical continuous-feed device, to replace hand feeding of the aluminum onto the filament, will improve coating uniformity.

To increase coating thickness, we used three twisted strands of 0.020-in.-diam aluminum wire in 205- and 405-min runs with a tungsten filament temperature of  $\sim 1650^\circ\text{C}$ . Metallography indicated coating thicknesses of  $< 2\ \mu$  for the beads coated for 205 min and  $< 3\ \mu\text{m}$  for the beads coated for 405 min. These coated particles are shown in Fig. 16. To increase coating thickness, we coated one lot of redeuterided  $\text{LiD}$  for a total of 560 min; 240 min with 0.08-in.-diam wire and 320 min with 0.02-in.-diam wire. A sample of this coated powder exposed to air for seven days showed no evidence of reaction when viewed at  $\sim 60\times$ . Metallography showed that coating thickness varied from  $\sim 3$  to  $6\ \mu$  and that the coating was solid. This coated powder is shown in Fig. 17. The photomicrograph at  $1000\times$  shows the grain structure of the  $\text{LiD}$  particle.

Powder originally spheroidized at  $1150^\circ\text{C}$  was passed through the drop tower again at 1075, 1090, or



70 min.



75 min.



126 min.

Fig. 11.

*LiD coated using 0.080-in.-diam aluminum wire, tungsten filament temperature 1650°C. 500X.*

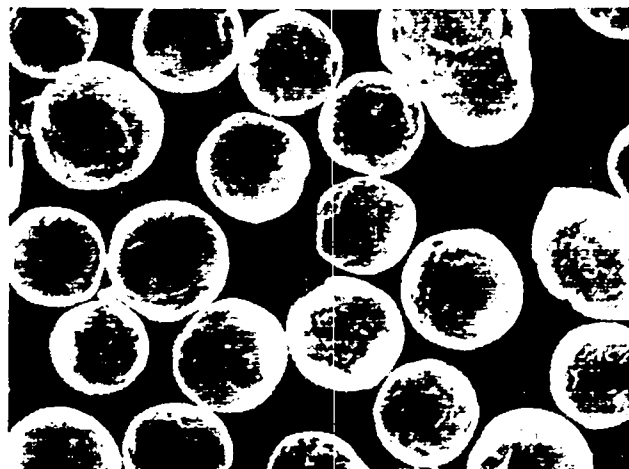


Fig. 12.

Radiograph of aluminum-coated redeuterided LiD. 100X.

1175°C in an attempt to improve the surface of the spheroidized particles, and evaluated by a scanning electron microscope (SEM). A second pass through the drop tower produced no significant improvement of surface property, regardless of temperature. We investigated the effect on surface roughness of multiple passes through the drop tower using as starting material LiD that was originally spheroidized at 1150°C. Samples of this material after 1, 2, 3, or 4 passes through the drop tower at 1100°C were evaluated by SEM. The SEM micrographs are shown in Figs. 18-20. In Fig. 18, the initiation of reaction with air is evident on the relatively smooth surface after the first pass at 1100°C. In Fig. 19, one of the particles shows evidence of increased reactivity after the second pass at 1100°C, probably because of more than average substoichiometric composition. After the third pass at 1100°C, the particles showed uniform surface characteristics. All of the particles subjected to the fourth pass had uniformly rough surfaces, probably because of the increased reactivity due to the more substoichiometric composition.

More studies will be required to improve surface quality; these include the effects of varying the length and temperature of the hot zone and the mechanical abrasion of particle surfaces.

UNCLASSIFIED



1000X.



1000X.



3000X.



3000X.

Fig. 13.

Glass beads coated using 0.080-in.-diam aluminum wire.

Fig. 14.

Glass beads coated using 0.020-in.-diam aluminum wire.

UNCLASSIFIED



UNCLASSIFIED

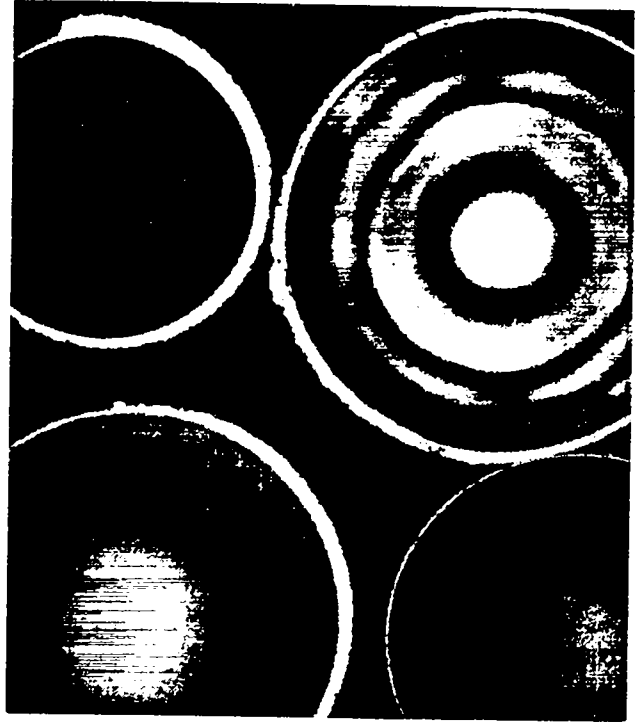
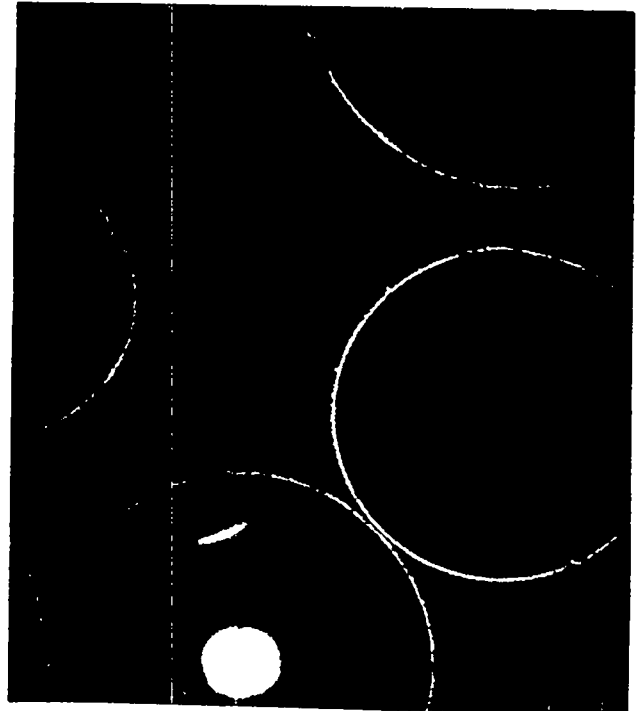
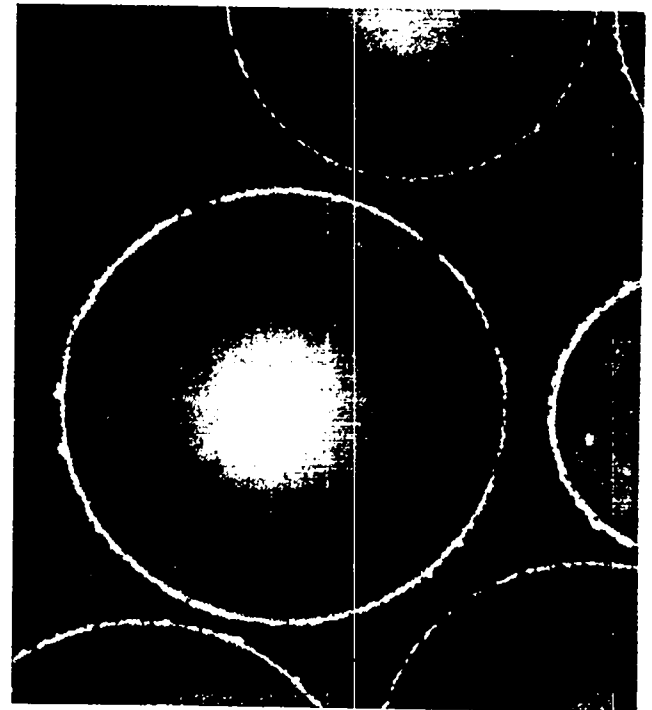


Fig. 15.  
 Aluminum-coated glass beads. 500X.

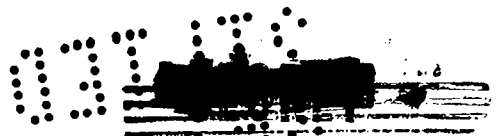


205-min coating time.



405-min coating time.

Fig. 16.  
 Glass beads coated using 0.020-in.-diam aluminum wire, tungsten filament temperature 1650°C. 500X.



UNCLASSIFIED



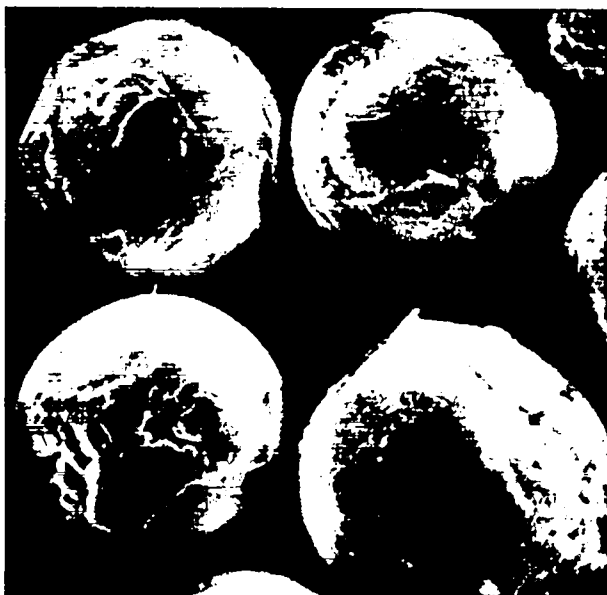
500X.



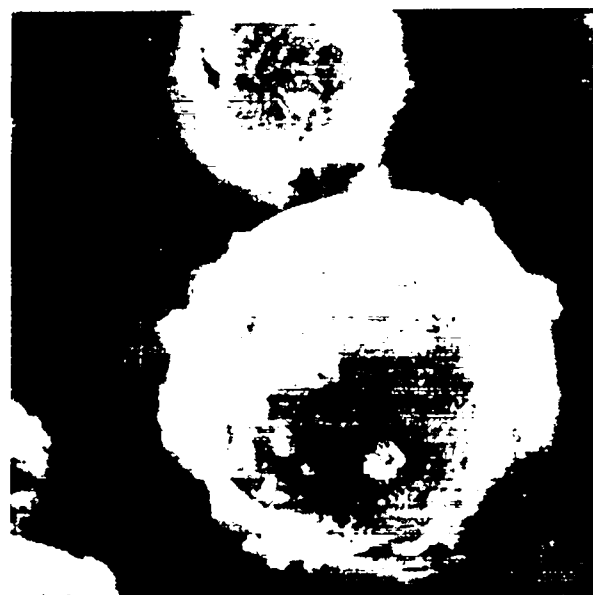
1000X.

Fig. 17.

*LiD coated using 0.020- and 0.080-in.-diam aluminum wire for 560 min, tungsten filament temperature 1650°C.*



Spheroidized at 1150°C.



First pass at 1100°C.

Fig. 18.

*SEM micrographs of LiD spheroidized at 1150°C after one pass through tower at 1100°C 300X.*



Fig. 19.

SEM micrographs of LiD after second (top) and third (bottom) pass through the drop tower at 1100°C. 300X.



Fig. 20.

SEM micrograph of LiD after fourth pass through the drop tower at 1100°C. 300X.

#### V. Progress Evaluation and Future Plans

The objectives of this program were to investigate the feasibility of spheroidizing LiH or LiD particles of uniform size; to restore the hydrogen lost during spheroidizing; and, ultimately, to coat these rejuvenated particles with a uniform coating of a metal such as aluminum. We have demonstrated the feasibility of meeting these objectives, but it becomes quite clear that quality must be improved at all stages of processing. This can be accomplished only by upgrading the facility so that the product will have gone through all processing steps in a closed-loop, high-purity, inert atmosphere system. Such a system involves a simple drybox train, wherein the lump LiD is admitted to the first box through a vacuum/argon atmosphere transfer-lock system. The lump LiD will be crushed and screened to yield particles of a very narrow particle-size range such as 95 to 105  $\mu\text{m}$ . The classified powder will then be transferred through locks to the next drybox where it will be spheroidized by dropping through a resistance-heated drop tower. The drybox atmosphere will be purified argon, and temperature will probably range from 1125 to 1175°C. This step, of course, is a major improvement over present practice and should yield a much improved product. The drop-tower product will

UNCLASSIFIED

again be passed through locks to the next drybox where the spherical particles will be separated from the nonspherical ones. The nonspherical particles will be sent back for spheroidizing. The spheroidized particles will be transferred as before to the next drybox where they will be redeuterided. Finally, the redeuterided particles will be transferred to the last drybox in the train where they will be coated. This step is considered to require major effort to provide reliable coating on a reproducible basis. Initial coating will be laid down by vacuum evaporation of aluminum. Eventually, this drybox will be equipped with a sputtering-type plating system that will permit a variety of materials to be deposited. An additional drybox can be added to the train to permit final coating of these metal-coated spheres with a plastic film. This entire operation is unique in that it can be accomplished with conventional materials, equipment, and processes. Some line-item equipment will be needed to make this system fully operative.

#### Acknowledgments

Many people have assisted us in this program, specifically J. Kostacopoulos crushed and screened the

bulk LiD and classified spherical from nonspherical powder; L. Tellier spheroidized the powders, and D. Carroll did the coating work. All of the above are members of the CMB-6 Powder Metallurgy Section. We also thank T. I. Jones and C. Javorsky of the CMB-6 Physical Metallurgy Section for the conventional metallography, T. Gregory of Group GMX-1 for the scanning electron micrographs, J. Langham for particle photography, and Group CMB-1 for the chemical analysis.

#### References

1. The LASL Advanced Propulsion Task Group, "Nuclear Pulsed Propulsion Study (U)," Los Alamos Scientific Laboratory report LA-4684-MS (SRD) (May 1971).
2. Mueller, Blackledge, and Libowitz, *Metal Hydrides*, Academic Press (1969).
3. C. E. Messer, "A Survey Report on Lithium Hydride," Tufts College, NY 09470, p. 3 (1960).

KT/ph:40

16

UNCLASSIFIED



UNCLASSIFIED

UNCLASSIFIED

